3D Bilateral Filtering of Cardiac DT-MRI Data

Tomasz Pieciak

AGH University of Science and Technology, Krakow, Poland

Abstract

In this paper, the 3D bilateral filtering (3DBF) method of cardiac diffusion tensor magnetic resonance imaging (DT-MRI) data is proposed. The technique integrates information both coming from spatial localization of the diffusion tensors (DTs) as well as angular similarity (AS) of primary eigenvectors of DTs and Jensen-Bregman LogDet (JBLD) divergence for covariance matrices.

In comparison to recently literature reports, we show that using a similarity measure based solely on a covariance matrices is not enough to perform the most accurate DT-MRI data enhancement in tensors domain.

Our investigation on synthetic and real ex-vivo canine cardiac DT-MRI data shows that the best results by 3DBF method are commonly obtained by AS measure and JBLD divergence synergy. The fractional anisotropy root mean-squared error (FA RMSE) for cardiac data decreased from 0.0855 *(noisy data) to* 0.0473*, whereas primary eigenvectors angle difference mean (AD) improved from* 25.9 ± 19.8 *to* 19.2 ± 18.9*.*

1. Introduction

DT-MRI is a modern and emerging medical imaging modality, which, as the only one, can assess fiber structure arrangement on a microscopic level in a non-invasive way [1, 2]. However, inherent cardiac cycle, respiratory system as well as technical issues (e.g., eddy currents, magnetic field inhomogeneity, Johnson-Nyquist noise) considerably affect the data quality [3], in particular change the directions of the principal eigenvectors and eigenvalues proportions of the diffusion tensors. In consequence, it leads to ambiguities in quantitative analysis of DTs (e.g., fractional anisotropy measure – FA) and fiber tracts obtained with tractography algorithms [4–7].

Although the diffusion data filtering process could be realized either on diffusion-weighted images (DWI) [7] or DT-MRI data [9], nevertheless, there is still no "gold standard" in this field. A comprehensive comparison of cardiac DT-MRI data enhancement techniques could be found in [6].

In this paper, however, we focus on the latter case and propose the filtering method to enhance the DT-MRI cardiac data quality, which operates directly on the tensor field and its properties. The paper is organized as follows. In section 2, the validity of this work is confirmed based on Monte Carlo simulations. Afterwards, in section 3, the filtering approach is presented and in section 4, numerical results of 3DBF are shown and compared. Finally, in the last part of the article, the concluding remarks are drawn.

2. Noise influence Monte Carlo simulation

To affirm validity of this work, we performed acceptance-rejection quasi-Monte Carlo (qMC) simulation with low-discrepancy Halton sequence and $M = 10000$ iterations for each noise standard deviation σ case. We chose $S_0 = 250$ amplitude with negligible small diffusion gradient, b-value fixed at $1000\ s/mm^2$ and six non-collinear diffusion gradient directions, which three of them are aligned to X, Y and Z axis, respectively. The diffusion attenuations were prepared in such a way that the primary eigenvector $\mathbf{v}_1 = [1, 0, 0]^T$ of the diffusion tensor is aligned with X axis. We generated artificial uncorrelated, between gradient directions, $\mathcal{N}(0; \sigma^2)$ distributed noise in real and imaginary parts of DWI data (equivalent to Rician distributed amplitude), reconstructed the DWI amplitudes and estimated DTs by weighted-least squares procedure [1]. To perform quantitative analysis of the deformed DT, the azimuthal $\Delta\theta$ and zenithal mean angle changes $\Delta\varphi$ of distorted primary eigenvector $\mathbf{v}_1' = \left[v_{1,x}', v_{1,y}', v_{1,z}'\right]^T$ were defined as:

$$\Delta\theta = \arccos\left(\frac{|v_{1,x}'|}{\|\widehat{\mathbf{v}}_1'\|}\right) \tag{1}$$

$$\Delta\varphi = \frac{\pi}{2} - \arccos\left(\frac{|v_{1,z}'|}{\|\mathbf{v}_1'\|}\right) = \arcsin\left(\frac{|v_{1,z}'|}{\|\mathbf{v}_1'\|}\right) \tag{2}$$

where $\widehat{\mathbf{v}}_1' = \left[v_{1,x}', v_{1,y}', 0\right]^T$ is $\mathbf{v}_1'$ projected onto XY plane and $\|\cdot\|$ is ℓ^2 vector norm.

In Fig. 1 qMC simulation results of $\Delta\theta$ and $\Delta\varphi$ mean changes are shown. For tensors, which represent similar to isotropic environment (FA=0.09), even the smallest noise

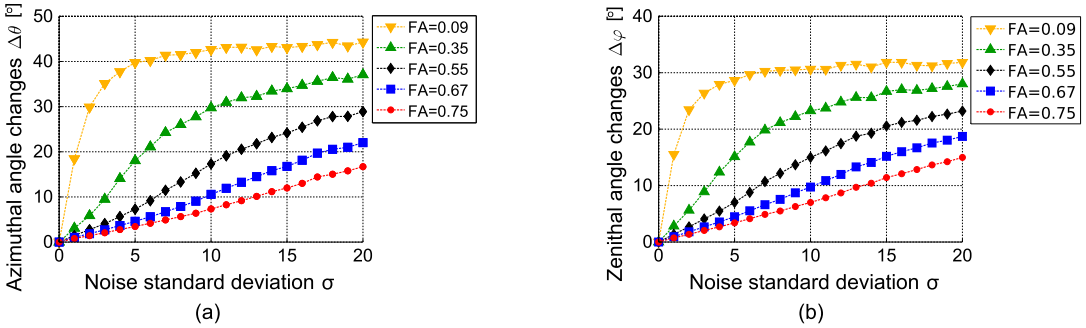

Figure 1. Comparison of azimuthal $\Delta\theta$ (a) and zenithal angle mean changes $\Delta\varphi$ (b) of primary eigenvector $\mathbf{v}_1$ of the diffusion tensor due to noise standard deviation σ and various tensors characterized by FA parameter

impact can radically change primary eigenvector direction. In fact, this is caused by possibility of eigenvalues proportions modification. The previous primary eigenvalue is no longer the biggest one, thus, the other eigenvector, associated with new dominant eigenvalue, indicates new major tensor direction. The zenithal angle mean changes $\Delta\varphi$ look analogously to $\Delta\theta$, however, slightly lower values of $\Delta\varphi$ are directly caused by the zenithal angle changes definition (2). For large FA value (FA=0.75), which represents highly anisotropic diffusion environment, both $\Delta\theta$ and $\Delta\varphi$ changes are featured by almost linear response in consideration of increasing noise standard deviation σ.

3. The 3D bilateral filtering algorithm

The bilateral filtering approach for grey and colour images was proposed in [8] and reinvestigated to diffusion tensor data in [9]. The bilateral filtering can be treated as a Nadaraya-Watson kernel estimator with adaptive selected weights, which depend not only on kernel choice and geometric closeness (distance) but also on diffusion tensors similarity. Following the notation included in [8], the bilateral filtering process for certain $\mathbf{x} \in \Omega$ ($\Omega \subset \mathbb{R}^3$) is defined as follows:

$$\widehat{\mathbf{D}}^{\mathbf{x}} = \int_{\Omega} w_D(\boldsymbol{\xi}, \mathbf{x}) w_S(\mathbf{D}^{\boldsymbol{\xi}}, \mathbf{D}^{\mathbf{x}}) \mathbf{D}^{\boldsymbol{\xi}} \, \mathrm{d}\boldsymbol{\xi} \tag{3}$$

where w_D and w_S are geometric closeness and diffusion tensor similarity normalized weights, respectively.

In this paper, we propose geometric closeness measure as an appropriately scaled cosine window:

$$w_D(\boldsymbol{\xi}, \mathbf{x}) = \begin{cases} \cos\left(\frac{\pi}{2} \cdot \frac{\|\boldsymbol{\xi}-\mathbf{x}\|}{\boldsymbol{\xi}_{\mathrm{MAX}}}\right) & \text{if } \|\boldsymbol{\xi}-\mathbf{x}\| < \boldsymbol{\xi}_{\mathrm{MAX}} \\ 0 & \text{otherwise} \end{cases} \tag{4}$$

whereas DTs similarity measure we define in the cut-off cosine window:

$$w_S^{(1)}(\mathbf{D}^{\boldsymbol{\xi}}, \mathbf{D}^{\mathbf{x}}) = \begin{cases} \cos\left(\frac{\pi}{2} \cdot \frac{\varphi}{\varphi_{\mathrm{MAX}}}\right) & \text{if } \varphi < \varphi_{\mathrm{MAX}} \\ 0 & \text{otherwise} \end{cases} \tag{5}$$

where φ is angle module between primary eigenvector $\mathbf{v}_1^{\mathbf{x}}$ of DT at given point $\mathbf{x}$ and its neighbourhood DT's primary eigenvector $\mathbf{v}_1^{\boldsymbol{\xi}}$:

$$\varphi = \arccos\left(\frac{|\langle \mathbf{v}_1^{\mathbf{x}}, \mathbf{v}_1^{\boldsymbol{\xi}} \rangle|}{\|\mathbf{v}_1^{\mathbf{x}}\| \|\mathbf{v}_1^{\boldsymbol{\xi}}\|}\right) \tag{6}$$

where $\langle \bullet, \bullet \rangle$ is an inner product and $\varphi_{\mathrm{MAX}} \in \left(0; \frac{\pi}{2}\right]$ is angle cut-off value. Henceforth, $w_S^{(1)}$ similarity measure we call angular similarity (AS). Also, we make use of recent proposed in literature Jensen-Bregman LogDet divergence for covariance matrices [10]:

$$d_{JBLD}(\mathbf{D}^{\boldsymbol{\xi}}, \mathbf{D}^{\mathbf{x}}) = \log\left|\frac{\mathbf{D}^{\boldsymbol{\xi}} + \mathbf{D}^{\mathbf{x}}}{2}\right| - \frac{1}{2}\log\left|\mathbf{D}^{\boldsymbol{\xi}}\mathbf{D}^{\mathbf{x}}\right| \tag{7}$$

where $|\bullet|$ is a determinant of a matrix, $\mathbf{D}^{\boldsymbol{\xi}}$ and $\mathbf{D}^{\mathbf{x}}$ are positive-semidefinite covariance matrices of diffusion tensors at $\boldsymbol{\xi}$ and $\mathbf{x}$ points, respectively.

Finally, the JBLD similarity measure we define as:

$$w_S^{(2)}(\mathbf{D}^{\boldsymbol{\xi}}, \mathbf{D}^{\mathbf{x}}) = \frac{2\widetilde{\mathbf{x}}}{1 + \exp\left(-\beta\left(\widetilde{\mathbf{x}} - d_{JBLD}(\mathbf{D}^{\boldsymbol{\xi}}, \mathbf{D}^{\mathbf{x}})\right)\right)} \tag{8}$$

with

$$\widetilde{\mathbf{x}} = \underset{\boldsymbol{\xi}:\ \|\boldsymbol{\xi}-\mathbf{x}\|<\boldsymbol{\xi}_{\mathrm{MAX}}}{\mathrm{median}} \left\{ d_{JBLD}(\mathbf{D}^{\boldsymbol{\xi}}, \mathbf{D}^{\mathbf{x}}) \right\} \tag{9}$$

However, an ordinary Euclidean averaging of DTs in (3) leads to a specific "swelling effect", in which averaged tensor has greater volume than components. Thus, we take advantage of *P*-average for DTs [11], whereby calculations are performed in a vector space (DTs form only a convex half-cone), and then modify (3) as follows:

$$\widehat{\mathbf{D}}^{\mathbf{x}} = \left(\int_{\Omega} w_D(\boldsymbol{\xi}, \mathbf{x}) w_S(\mathbf{D}^{\boldsymbol{\xi}}, \mathbf{D}^{\mathbf{x}}) \left(\mathbf{D}^{\boldsymbol{\xi}}\right)^p \, \mathrm{d}\boldsymbol{\xi} \right)^{\frac{1}{p}} \tag{10}$$

Table 1. 3DBF results with AS, JBLD and AS+JBLD similarity measures on synthetic DT-MRI dataset (Fig. 2a, 16x16x16 lattice) due to various noise standard deviation σ in complex DWI domain. Best results for fixed σ value are bolded

Noise	Fractional anisotropy RMSE					Angle difference mean $\pm$ std. dev. [°]				
σ	Noisy	AS	JBLD	AS+JBLD	H&H	Noisy	AS	JBLD	AS+JBLD	H&H
5	0.0735	0.0148	0.0201	**0.0146**	0.0490	8.7 ± 4.9	1.9 ± 2.2	2.1 ± 1.6	**1.8** ± 2.2	3.4 ± 5.4
10	0.1508	0.0506	0.0547	**0.0476**	0.0613	18.6 ± 12.9	5.4 ± 8.8	5.7 ± 4.8	**4.9** ± 6.6	5.5 ± 5.7
15	0.2167	0.1236	0.0779	**0.0776**	0.0830	27.1 ± 17.6	12.1 ± 14.1	8.8 ± 7.9	8.5 ± 9.2	**7.6** ± 8.7
20	0.2538	0.1556	0.0906	**0.0888**	0.0921	33.8 ± 20.8	19.1 ± 18.4	12.0 ± 8.8	12.2 ± 12.2	**10.4** ± 7.0

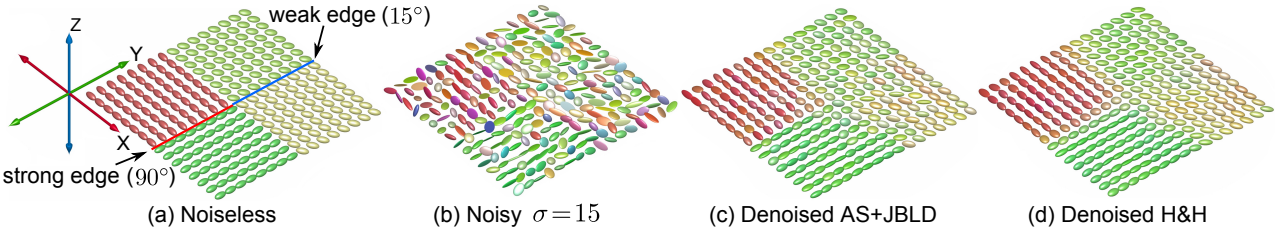

(a) Noiseless (b) Noisy $\sigma = 15$ (c) Denoised AS+JBLD (d) Denoised H&H

Figure 2. 3DBF results with AS+JBLD measure compared to the H&H method [9] (d_{T_J} measure and $\alpha = 1$) on synthetic DT-MRI dataset. Pictures represent the single slices of noiseless (a), noisy (b) and denoised DTs fields (c, d), respectively

where

$$\left(\mathbf{D}^{\boldsymbol{\xi}}\right)^p = \mathbf{V}^{\boldsymbol{\xi}} \left(\boldsymbol{\Lambda}^{\boldsymbol{\xi}}\right)^p \left(\mathbf{V}^{\boldsymbol{\xi}}\right)^T \tag{11}$$

is an eigendecomposition of the tensor $\left(\mathbf{D}^{\boldsymbol{\xi}}\right)^p$ and $\left(\boldsymbol{\Lambda}^{\boldsymbol{\xi}}\right)^p$ is the diagonal matrix of an eigenvalues powers:

$$\left(\boldsymbol{\Lambda}^{\boldsymbol{\xi}}\right)^p = \operatorname{diag}\left[\left(\lambda_1^{\boldsymbol{\xi}}\right)^p, \left(\lambda_2^{\boldsymbol{\xi}}\right)^p, \left(\lambda_3^{\boldsymbol{\xi}}\right)^p\right], \quad p \in \mathbb{R}_+ \tag{12}$$

4. Numerical results

We conducted experiments both on synthetic and real *ex-vivo* canine cardiac DT-MRI datasets (description of the cardiac data is included in [5]). To confirm performance of the proposed method, we generated artificial $\mathcal{N}(0; \sigma^2)$ distributed noise in complex domain of DWI data. Then, we tested the proposed method with AS, JBLD, and AS+JBLD similarity measures variants and compared the obtained results with those from method proposed in [9] with d_{T_J} measure and $\alpha = 1$ (denoted in this article as H&H). Experiments on real cardiac DT-MRI data were preceded by a beforehand DWI data denoising by well-known from image processing literature Perona&Malik filter [12], thus, artifical Rician noise can be applied and quantitative parameters differences calculated between *noiseless* and denoised datasets. In AS+JBLD case, we extend the definition (10) by additional similarity weighting component $w_S = \gamma w_S^{(1)} + (1-\gamma) w_S^{(2)}$. For all of our experiments on synthetic dataset we chose $\boldsymbol{\xi}_{\mathrm{MAX}} = 4$, $\varphi_{\mathrm{MAX}} = \pi/3$, $\beta = 100$, $\gamma = 1/10$ and $p = 1/10$ as suggested in [11], whereas on real cardiac DT-MRI data we assumed $\varphi_{\mathrm{MAX}} = \frac{4\pi}{9}$ and $\gamma = 1/3$.

Our investigation shows that the lowest fractional anisotropy root mean-squared errors (FA RMSEs) between noiseless and denoised tensors are reached in AS measure and JBLD divergence synergy (Table 1, Fig. 1, Fig. 2). Moreover, introducing an additional similarity component (AS+JBLD), we commonly obtain more reliable representation of anisotropy than separately using either AS or JBLD divergence as a diffusion tensor similarity measure. The lowest primary eigenvectors angle difference mean (AD) between noiseless and denoised tensors for low ($\sigma = 5$) and medium noise level ($\sigma = 10$) are reached in AS+JBLD measure. However, for high noise standard deviation ($\sigma \geq 15$), the 3DBF is still eclipsed by the H&H method, especially in primary eigenvectors $\mathbf{v}_1$ restoration accuracy (Table 1). Furthermore, 3DBF approach has an intrinsic drawback. If the noise highly distorts the data close to the edge, the damaged DT will not be recreated into the initial state in a single iteration of the algorithm. Nevertheless, the H&H approach has also an imperfection, e.g., the algorithm smooths strong edges (Fig. 2d).

In addition, we notice that high angle similarity cut-off value selection (e.g., $\varphi_{\mathrm{MAX}} = \pi/3$) leads to the most accurate results of the AS+JBLD variant, notably for very high noise standard deviation ($\sigma = 20$). However, permanently increasing φ_{MAX} value reflects wide range of different DTs in averaging process, hence, the filtering procedure blurs strong (90° between adjacent primary eigenvectors) and weak (15°) edges as well as other featured information.

5. Conclusion and remarks

The 3DBF with AS+JBLD measure approach allows one to significant enhance cardiac DT-MRI data, therefore, the FA parameter and principal eigenvectors field could be

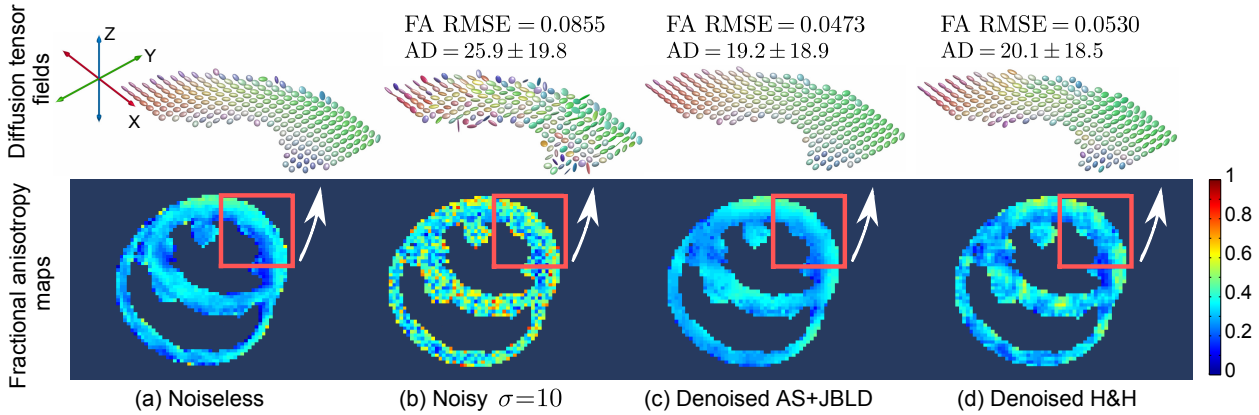

Figure 3. Diffusion tensor fields and fractional anisotropy parameter maps of noiseless (a), noisy (b) and denoised cardiac DT-MRI data (080803) by the proposed method with AS+JBLD measure (c) and compared to H&H approach (d).

reflected in a more credible way. However, we note that for tractography data preprocessing (primary eigenvectors recovery task) and high noise level ($\sigma \geq 15$), it makes sense to use H&H method.

We call attention to the feature preservation of our method, therefore, strong DT edges are kept (Fig. 2c). Furthermore, the approach defined as (10) does not require special treatment of the boundaries and could be integrated for more accurate image segmentation process of the heart (e.g., generalization of active contour method into tensor domain [9, 13, 14]).

Acknowledgements

This work is founded by the AGH University of Science and Technology as a research project No. 11.11.120.612. We are thankful to Drs. Patrick A. Helm and Raimond L. Winslow at the Center for Cardiovascular Bioinformatics and Modeling and Dr. Elliot McVeigh at the National Institute of Health for provision of data as well as Ghassan Hamarneh for sharing the source code of H&H method for performance comparisons.

References

[1] Basser PJ, Mattiello J, LeBihan D. Estimation of the Effective Self-Diffusion Tensor from the NMR Spin Echo. J. Magn. Reson., Ser B 1994;103:247–54

[2] LeBihan D, Mangin JF, Poupon C, Clark CA, Pappata S, Molko N, Chabriat H. Diffusion Tensor Imaging: Concepts and Applications. J Magn Reson Imaging 2001;13:534–46

[3] Wei H, Viallon M, Delattre B, Wang L, Pai VM, Wen H, Xue H, Guetter Ch, Croisille P, Zhu Y. Assessment of cardiac motion effects on the fiber architecture of the human heart in vivo. IEEE Trans Med Imag 2013 (to appear)

[4] Basser PJ, Pajevic S. Statistical Artifacts in Diffusion Tensor MRI (DT-MRI) Caused by Background Noise. Magnet Reson Med 2000;44:41–50

[5] Pieciak T. Bootstrap Uncertainty Estimation of Canine Cardiac Fibers Anisotropy and Diffusivity on DT-MRI Data. Computing in Cardiology 2012;39:369–372

[6] Frindel C, Croisille P, Zhu YM. Comparison of regularization methods for human cardiac diffusion tensor MRI. Med Image Anal 2009;13:405–18

[7] Zhang Y, Liu W, Isabelle M, Yuemin Z. Feature-Preserving Smoothing of Diffusion Weighted Images Using Non-stationarity Adaptive Filtering. IEEE Trans Biomed Eng 2013;60:1693–701

[8] Tomasi C, Manduchi R. Bilateral Filtering for Gray and Color Images. ICCV 1998;839–46

[9] Hamarneh G, Hradsky J. Bilateral Filtering of Diffusion Tensor Magnetic Resonance Images. IEEE Trans Image Process 2007;16:2463–75

[10] Cherian A, Sra S, Banerjee A, Papanikolopoulos N, Efficient similarity search for covariance matrices via the Jensen-Bregman LogDet Divergence, ICCV 2011;2399–406

[11] Herberthson M, Brun A, Knutsson H. *P*-Averages of Diffusion Tensors. SSBA 2007

[12] Perona P, Malik J. Scale-space and edge detection using anisotropic diffusion, IEEE Trans Pattern Anal Mach Intell 1990;12:629–39

[13] Pieciak T. Myocardial Segmentation Based on Magnetic Resonance Sequences. Bio-Algorithms and Med-Systems 2010;6:85–90

[14] Pieciak T. Segmentation of the Left Ventricle Using Active Contour Method with Gradient Vector Flow Forces in Short-Axis MRI. Information Technologies in Biomedicine 2012;24–35

Address for correspondence:

Tomasz Pieciak
AGH University of Science and Technology
Al. Mickiewicza 30
30-059 Krakow
pieciak@agh.edu.pl